Report No. BMI-1387
UC-25 Metallurgy and Ceramics
(TID-4500, 15th Ed.)

Contract No. W-7405-eng-92

A VISUAL STUDY OF THE CORROSION OF DEFECTED ZIRCALOY-2-CLAD FUEL SPECIMENS BY HOT WATER

by

Elmer F. Stephan
Paul D. Miller
Frederick W. Fink

October 19, 1959

BATTELLE MEMORIAL INSTITUTE
505 King Avenue
Columbus 1, Ohio

DISCLAIMER

TABLE OF CONTENTS

A VISUAL STUDY OF THE CORROSION OF DEFECTED ZIRCALOY-2-CLAD FUEL SPECIMENS BY HOT WATER

Elmer F. Stephan, Paul D. Miller, and Frederick W. Fink

The failure of defected Zircaloy-2-clad uranium and uranium-2 w/o zirconium fuel specimens in high-purity high-pressure water at 200 to 345 C was observed in a windowed autoclave. Time-lapse color motion pictures were taken to provide a record of the progressive changes ending in the complete disintegration of the core material in the specimens. Continuous measurement of the pressure increase caused by accumulation of hydrogen served to monitor the progress of the reaction when clouding of the water by corrosion products made visual observation impossible.

The nature of the attack of all specimens was similar, although the time at which different stages occurred varied. Following an induction period, the first evidence of attack was the slow formation of a blister in the cladding area surrounding the defect. Eventually, a copious evolution of hydrogen occurred at the base of the swollen area. In general, a crack could be seen in the cladding at this stage. Catastrophic failure of the specimen followed swiftly.

The time required for each phase of the reaction was reduced as the temperature was raised. Initial swelling occurred after about 24 min at 345 C but only after 8 hr at 200 C. Diffusion-treated uranium-2 w/o zirconium-cored specimens were most resistant to attack. Specimens with beta-treated water-quenched natural-uranium cores were least resistant.

INTRODUCTION

All reactors provide some method for monitoring the activity of the coolant stream to check for fuel-element failures. This practice is based on the assumption that catastrophic failure of an element will be heralded by enough radioactivity in the coolant stream to be above the threshold level of the detection instrument. Little work has been done, however, in correlating fission-product activity in the coolant stream with the actual progress of corrosion. It would be of particular value to know the details of the processes which could occur if a pinhole should develop in the cladding. For example, a knowledge of the speed of the reaction and the characteristics of the failure would be quite useful.

In previous work at BMI[1] a windowed-autoclave technique was found to be very useful for following the progress of corrosion in situ. The procedure gives a better understanding of the role which cladding defects play in the corrosion process than is provided by the periodic inspection and weight-change data of the conventional corrosion test.

The present report describes the progress of failure in a number of Zircaloy-clad uranium and uranium-2 w/o zirconium fuel specimens in water of various

(1) References at end.

temperatures. The step-by-step disintegration of the element was observed continuously in a windowed autoclave by a time-lapse motion-picture technique. The primary concern of the study was a better understanding of the corrosion process rather than a quantitative evaluation of the effect of element geometry and core composition, although each of these factors was varied.

The progress of the corrosion as recorded by the motion pictures was monitored by simultaneous measurement of the hydrogen pressure generated by the reaction of uranium and water. These pressure measurements also provided information for the stage in the exposure where the progress of corrosion could no longer be followed visually.

The present report describes ten such corrosion experiments, grouped according to the exposure conditions.

EXPERIMENTAL WORK

Specimens

Time-lapse motion pictures in color were taken of the action of hot water on 13 different specimens. The specimens are described in Table 1. Most contained natural unalloyed uranium cores. The specimens varied in heat treatments, cladding thickness, and configuration. One contained a uranium-2 w/o zirconium-alloy core. All were clad with Zircaloy-2. The specimens were approximately 2 in. long. The rod specimens were approximately 0.6 in. in diameter, while the two tubular specimens were 1.2 in. in diameter. The defect was a 25-mil-diameter hole drilled through the cladding to the core material at the side of the specimen, midway between the end plates.

Apparatus and Procedure

The autoclave and associated apparatus used for studying the failure of clad fuel specimens are shown in Figure 1. The procedures used for obtaining the time-lapse motion pictures were developed previously and are described in detail in BMI-998.

Essentially, the apparatus consists of a windowed-autoclave system, shown in Figure 2, and an optical system for photographing and viewing the reaction as pictured in Figure 3. A cross-sectional sketch of the windowed autoclave showing the position and mounting of the specimen is presented in Figure 4. Illumination was furnished by a Bunton spotlight equipped with a General Electric 100G 16-1/2/29SC bulb. The time-lapse motion pictures were taken with a 16-mm Paillard Bolex H-16 movie camera having a 63-mm Ektanon Kodak lens and an external electric motor with a spring drive. A Semenco movie control, Model MC-5, was used to actuate the spotlight, motor, and solenoid tripper for exposing the picture frames at the desired intervals.

TABLE 1. DESCRIPTION OF FUEL-ELEMENT SPECIMENS

Specimen	Description
G-11, G-12, G-13, G-14, G-15, and G-22	Coextruded, natural uranium 0.6 in. in diameter with nominally 30-mil-thick Zircaloy-2 cladding; beta treated at 720 to 730 C for 10 min; water quenched to 590 to 600 C, held for 10 min; air cooled
G-16	Same as above except cladding machined to nominal 20-mil thickness
G-17	Same as above except cladding machined to nominal 10-mil thickness
C-8 and C9	Coextruded, natural uranium 0.62 in. in diameter with nominally 30-mil-thick Zircaloy-2 cladding; beta treated at 720 to 730 C for 10 min, water quenched
D-8	Coextruded uranium-2 w/o zirconium 0.9 in. in diameter with nominally 20-mil-thick Zircaloy-2 cladding; diffusion treated 5-1/2 hr at 860 C, water quenched
Tubular (two specimens)	Coextruded, natural uranium 1.2 in. in diameter with Zircaloy-2 cladding; beta treated as for G-series

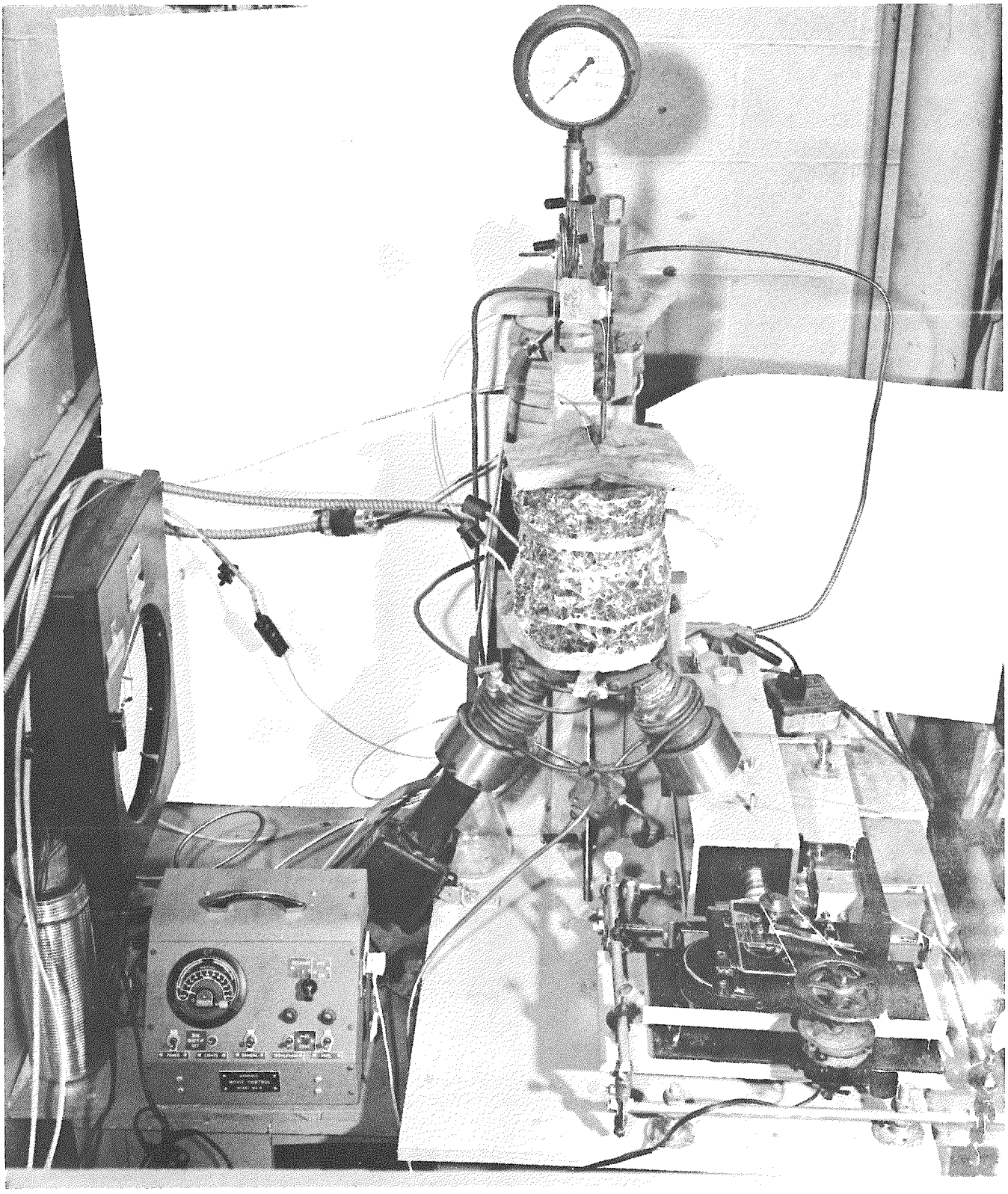

N59178

FIGURE 1. PHOTOGRAPH OF APPARATUS FOR OBSERVING THE CORROSIVE ACTION OF HOT WATER ON DEFECTED FUEL ELEMENTS

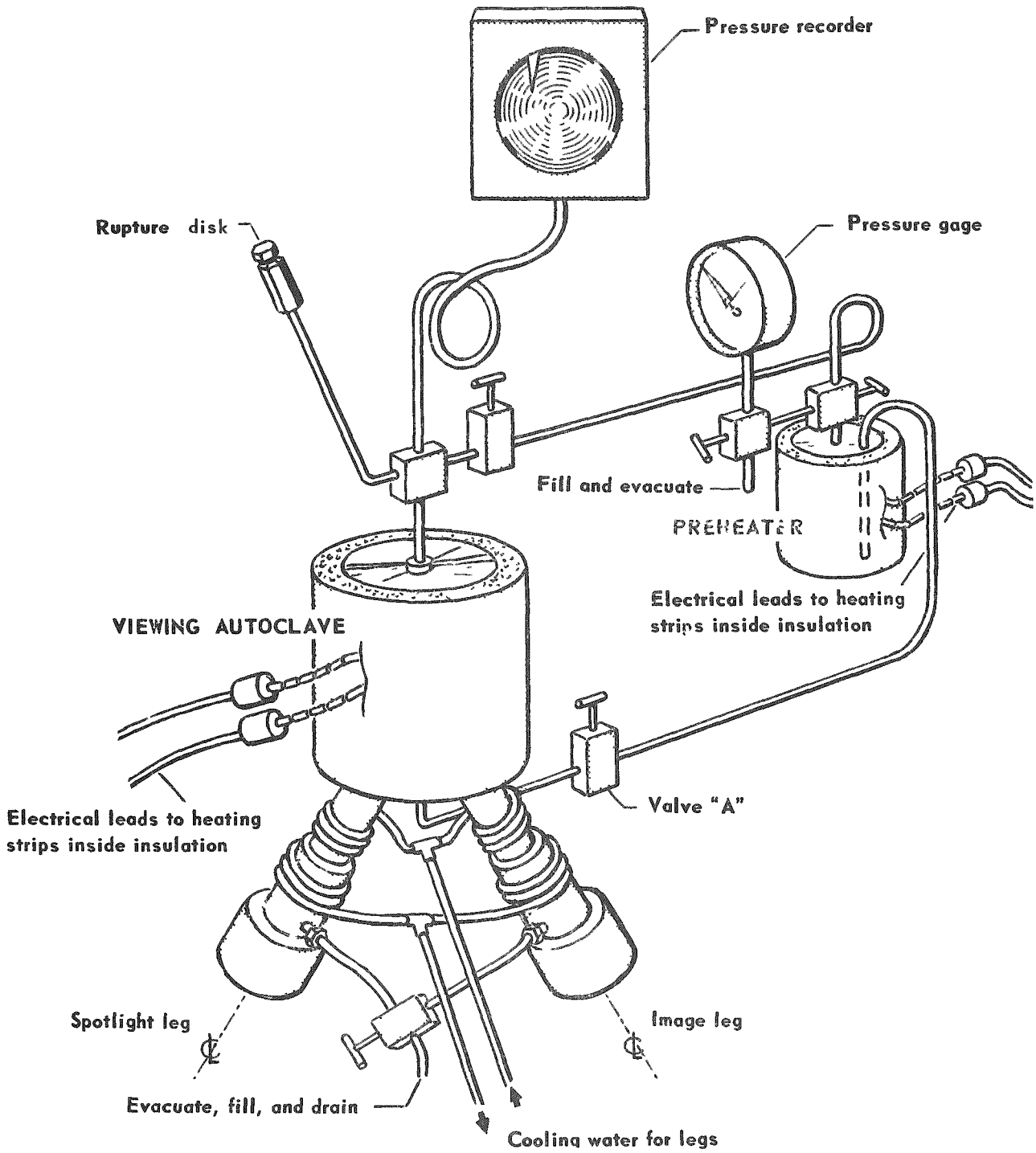

FIGURE 2. WINDOWED-AUTOCLAVE SYSTEM

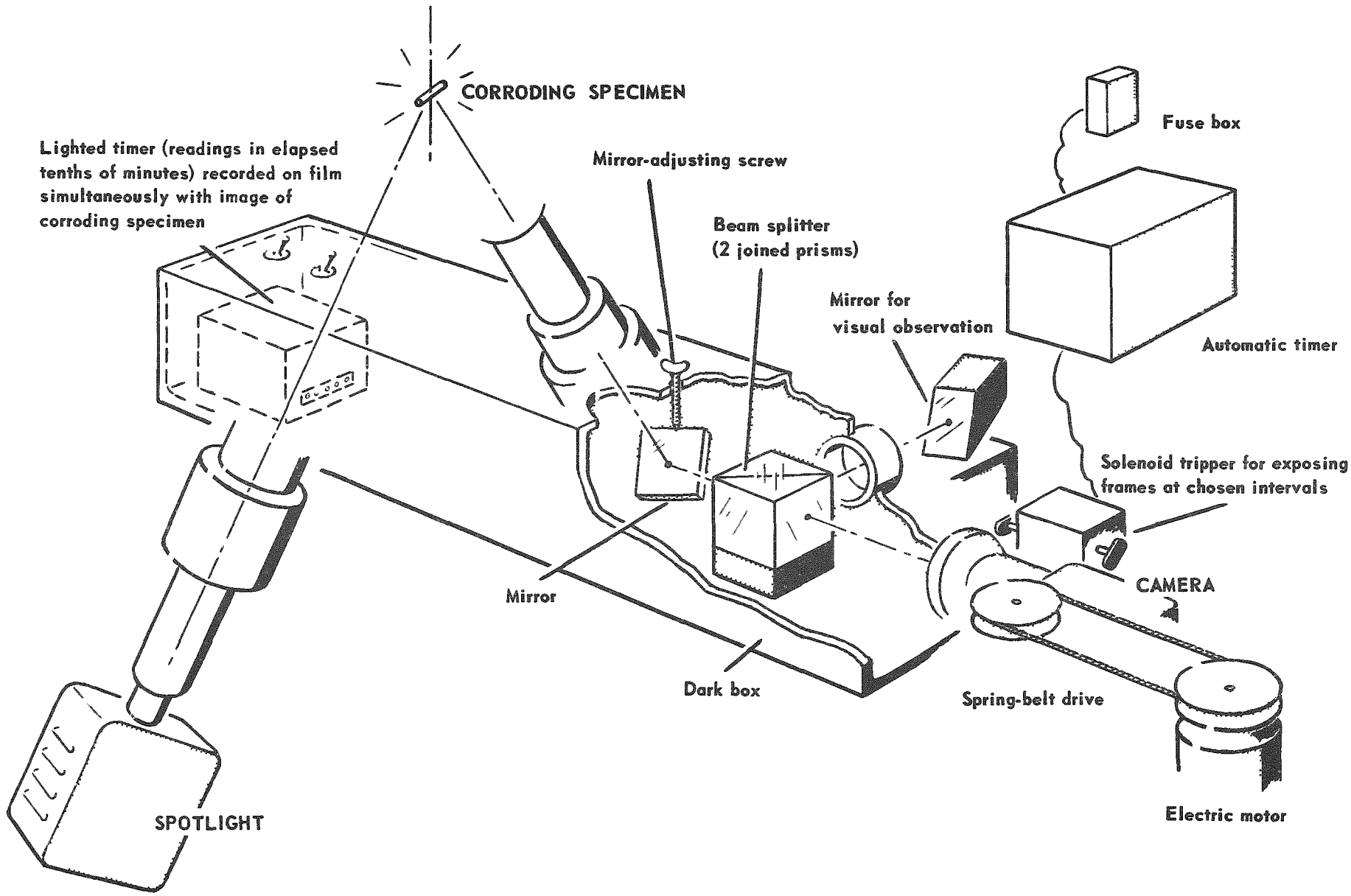

FIGURE 3. PHOTOGRAPHING AND OBSERVATION SYSTEM

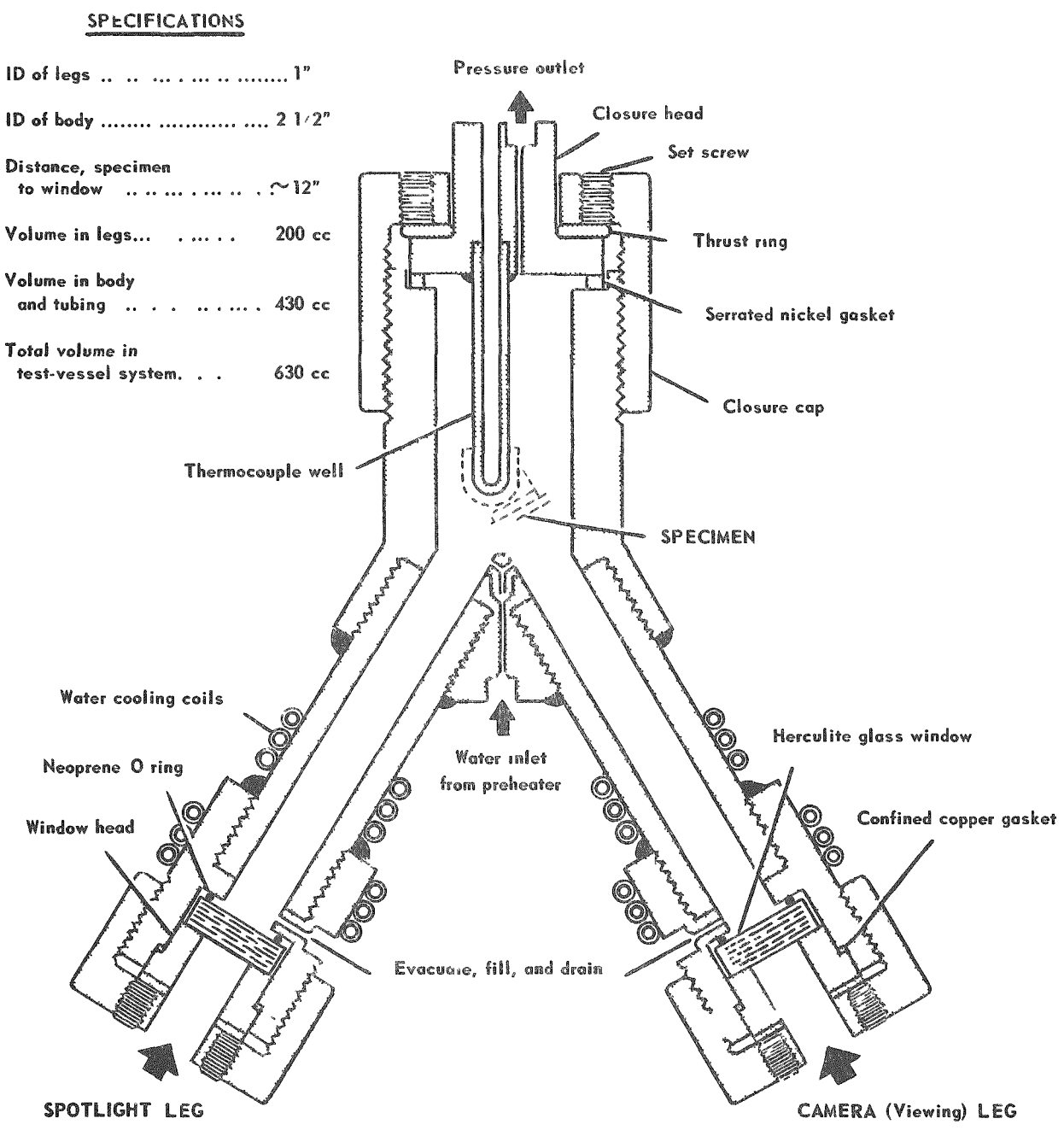

FIGURE 4. CROSS SECTION OF WINDOWED AUTOCLAVE

The specimen to be photographed was mounted against a gold plate which prevented reflections from the water-vapor interface. The camera was focused on the defect. This procedure allowed a 1-in.- diameter area surrounding the defect to be viewed. About 100 ml of cold water was admitted to the windowed leg sections of the autoclave, and the system was evacuated to degas the water. All water used in the tests was distilled and demineralized by Amberlite MB-2 mixed-bed ion-exchange resin. The resistivity was greater than 1×10^6 ohms. The autoclave section containing the specimen was heated to test temperature after which sufficient hot water was admitted to completely cover the specimen. The camera and running-time meter were started as the preheated water was introduced.

Experiments 1 and 2 were made with Kodachrome-A film. This was replaced by a much faster film, Super-Anscochrome Tungsten K 3200, for the remainder of the experiments. The faster film gave greater definition and extended the viewing time.

The frame speed and lens opening were varied according to the action as observed through the visual mirror. Generally, 1 frame per 10 sec was exposed until the swelling began, and then 1 frame per 4 sec was exposed during the swelling. Following the rupture of the cladding, exposure was again at the rate of 1 frame per 10 sec.

The changes in pressure in the autoclave were recorded continuously throughout each experiment. Since the pressure changes were caused primarily by the hydrogen evolved as a corrosion product, the time-pressure lag provided a measure of the speed and duration of corrosion.

Results

Photographic Study

The photographic record and the visual observation of the nature of the attack of the hot water at the defect showed that the corrosive action was similar for all the specimens examined. Wide variations were noted, however, in the times at which the various stages of failure occurred. The first evidence of attack was a slight dimpling of the cladding around the hole. As the action continued, this swelling expanded until a well-defined blister could be seen. The times at which the first detectable swelling could be seen with the various specimens are presented in Table 2, and are shown graphically in Figure 5.

The first evidence of a break in the cladding was the evolution of fine bubbles of hydrogen. The times for this occurrence also are recorded in Table 2.

Cracks could be seen almost simultaneously with the gas bubbles. It seems logical to assume that cracks in the cladding would precede the appearance of hydrogen bubbles. This suggests that cracks too small to be observed were present in the cladding where there appeared to be a delay between evolution of hydrogen and the first visible cracking. On the other hand, it should be noted that the cladding on Specimen D-8 ruptured 7 hr before gas evolution was observed. It is believed that the corrosion-resistant diffusion layer was partially responsible for the apparent slow appearance of hydrogen in this case.

TABLE 2. SUMMARY OF EXPERIMENTAL DATA FOR THE CORROSION OF DEFECTED COEXTRUDED ZIRCALOY-2-CLAD FUEL ELEMENTS BY HOT WATER

Experiment	Specimen[a]	Temperature, C	Time Interval to First Evidence of Action, hr				Total Pressure at Room Temperature After Complete Reaction, psi	Head Space, ml	Calculated Hydrogen Volume, STP, ml	Calculated Uranium From Hydrogen Evolved, g	Original Weight of Specimen, g	Final Weight of Specimen, g	Weight Loss (Core Material) by Difference, g
			Swelling	Gas Evolution	Cladding Rupture	Complete Reaction							
1	G-11	200	8	14.7	15.2	24	1300	265	21,470	114.2	151.5670	14.6190	136.9480
2	G-12	225	6	7.5	7.75	13	650	500	20,256	107.7	151.3530	16.1462	135.2068
4	G-13	250	1.7	2.5	2.75	10	300	1100	20,568	109.4	150.6603	18.3832	132.2771
3A[b]	G-14	300	1.0	1.5	1.5	4.75	260	1100	17,826	94.8	151.8375	32.2105	119.6270
3B	G-22	300	0.7	1.3	1.3	6.6	325	1140	23,072	122.7	151.6992	15.0711	136.6281
6	G-16	300	0.75	1.25	1.25	6.25	325	1100	22,750	119.1	149.0380	14.5895	134.4485
7	G-17	300	0.75	1.1	1.1	6.1	H_2 Leak	--	--	--	147.1103	11.2018	135.9085
8[b]	C-8	300	0.3	0.75	0.75	2.5	350	1140	24,865	132.3	174.5286	17.7234	156.8052
8B	C-9	300	0.3	0.70	0.70	3.5	350	1100	23,968	126.9	174.8296	18.9044	155.9252
9[c]	Tubular	300	0.5	0.9	0.9	5.5	600	1200	22,600[d] 44,500	358.0	397.655	31.630	366.025
9B	Tubular	300	0.3	0.55	0.55	4.0	H_2 Leak	--	--	--	336.550	24.237	312.213
5	G-15	345	0.4	0.8	0.8	3.2	250	1200	18,698	100.0	151.1303	16.5844	134.5459
10	D-8	300	24	48	41	54	450	1200	24,364[d] 33,667	311	362.682	27.378	335.304

(a) See Table 1 for description of specimens.

(b) Films for these two specimens were found to be underexposed. Repeat runs, Experiments 3B and 8B, were then made.

(c) Malfunction of the running-time meter occurred in Experiment 9, and a crack unexpectedly developed in the Zircaloy cladding. A repeat run, Experiment 9B was then made.

(d) Hydrogen bled off during the reaction.

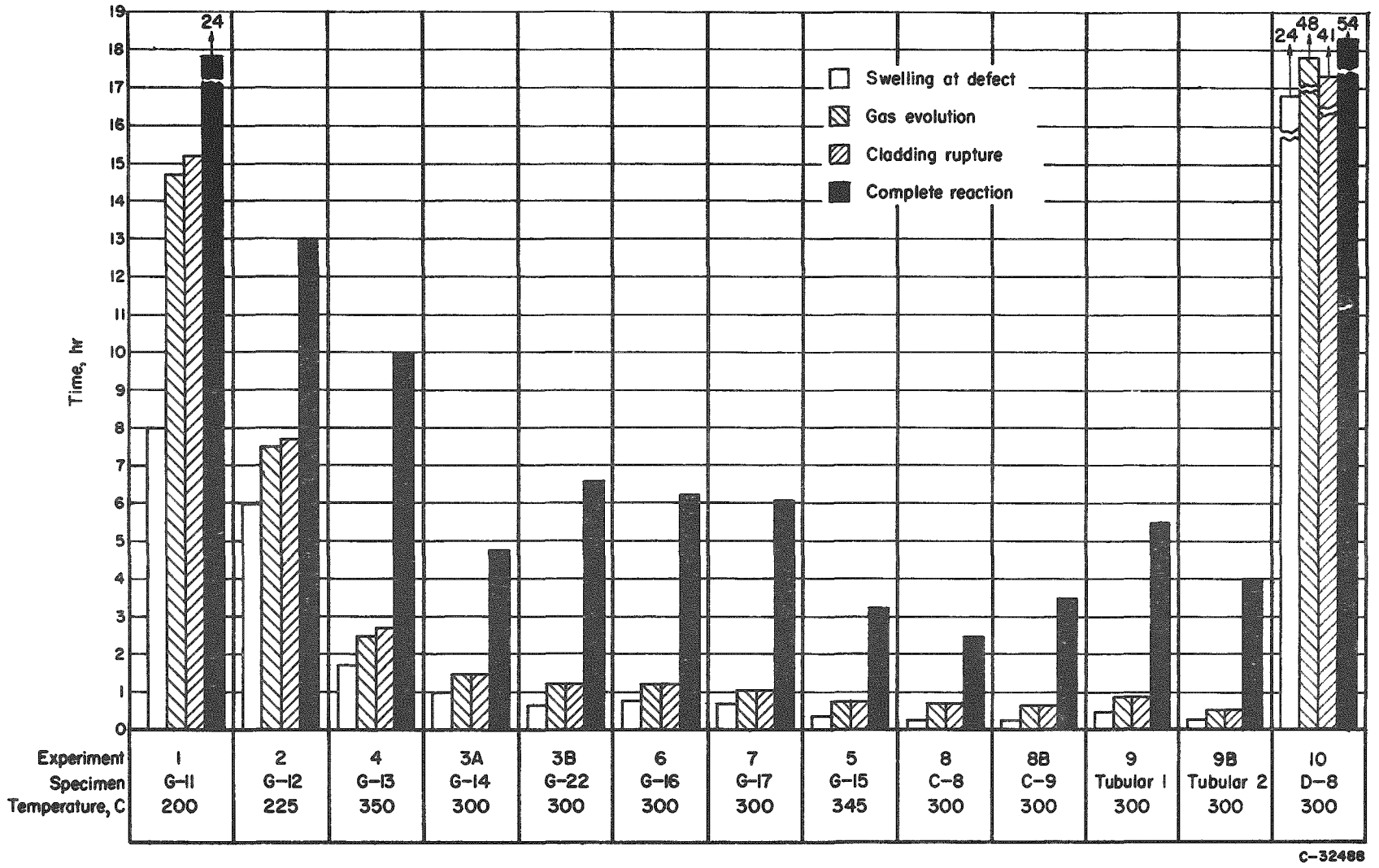

FIGURE 5. SUMMARY OF OBSERVED ACTION VERSUS TIME FOR THE VARIOUS SPECIMENS AND EXPERIMENTAL CONDITIONS

As the attack progressed, the cracks widened and the entire swollen area was lifted until a large area of the core was exposed. Usually, the cracks developed about 1/8 to 1/4 in. from the defect. Only the thin-walled specimens, G-17 and D-8, cracked through the hole. With the possible exception of Experiment 1 at 200 C, at no time prior to the development of the cracks in the cladding was any corrosion product or gassing detected coming from the defect hole. As soon as the cladding cracked and the gas bubbles appeared, the black corrosion products from the core material began to stream out into the water. The action at first was slow, but the rate increased rapidly as the area of the cladding surrounding the defect was lifted. Within a short time after rupture, the particles of corrosion product covered the windows and interfered with the observation of the element to its complete destruction.

The completion of the reaction was taken to be the time at which no increase in pressure in the autoclave could be detected. It can be seen in Figure 5 that the reaction continued for fairly long times after cracking had occurred.

Typical examples of the action at various stages are shown in Figure 6. These photographs were reproduced from the film of Experiment 9B.

The appearance of the cladding shells remaining after the completion of the experiments is shown in Figure 7. It can be seen that the Zircaloy-2 cladding suffered extensive tearing and distortion. The expansion from the uranium oxide formed from corrosion probably provided the force to distort the cladding.

Films were obtained for ten fuel-element specimens. Although the films for Experiments 1 and 2 were underexposed, they showed some of the action. For the remaining eight films the photography was considerably improved. Various stages of the failure could be observed in detail.

An analysis of the data, shown by the films, by Figure 7, and by Table 2, indicates that several factors are of great importance in the failure of fuel elements. These can be summarized as follows:

(1) An increase in temperature from 200 to 345 C speeded decidedly the reaction of the rod elements containing natural uranium. For example, swelling occurred after 8 hr at 200 C and after 24 min at 345 C. The elements exposed at intermediate temperatures responded in a proportionate manner. Similarly, 24 hr was required for completion of the reaction at 200 C and only slightly more than 3 hr was required at 345 C.

(2) Cladding thickness had very little effect at any stage during the disintegration of Specimens G-22, G-16, and G-17.

(3) Tubular elements were somewhat less durable than rod elements of the same core material and cladding.

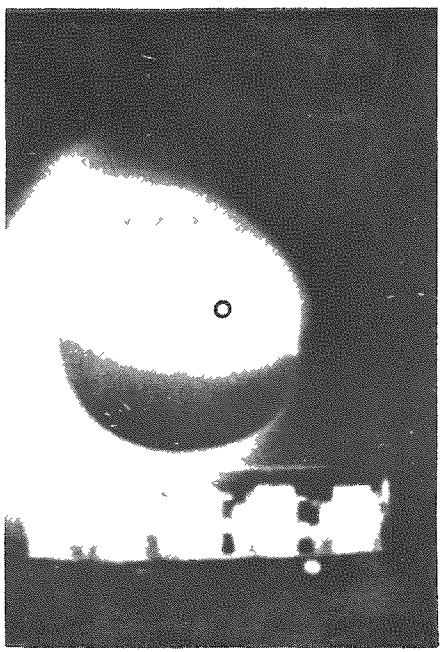

N61608

a. After 1.4 Min

Defect is encircled.

N61609

b. After 28.3 Min

Swelling of the cladding surrounding the defect may be seen.

N61610

c. After 36.6 Min

The cladding has ruptured at the base of the swelling. Hydrogen bubbles can be seen escaping from the rupture.

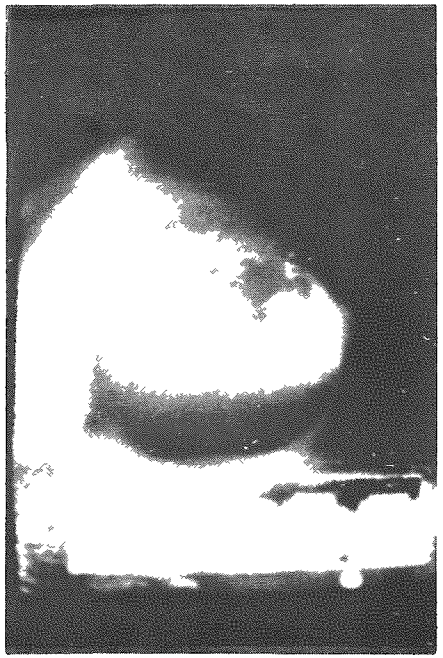

N61611

d. After 56.0 Min

The cladding surrounding the defect has been lifted back, exposing the core. Secondary swelling areas are occurring around the initial ruptured area. At this point the water is very dark due to suspended corrosion product. The exposure time was lengthened in order to view the specimen, which overexposed the running-time meter.

FIGURE 6. PROGRESS OF CORROSION IN A ZIRCALOY-2-CLAD ELEMENT EXPOSED TO 300 F WATER

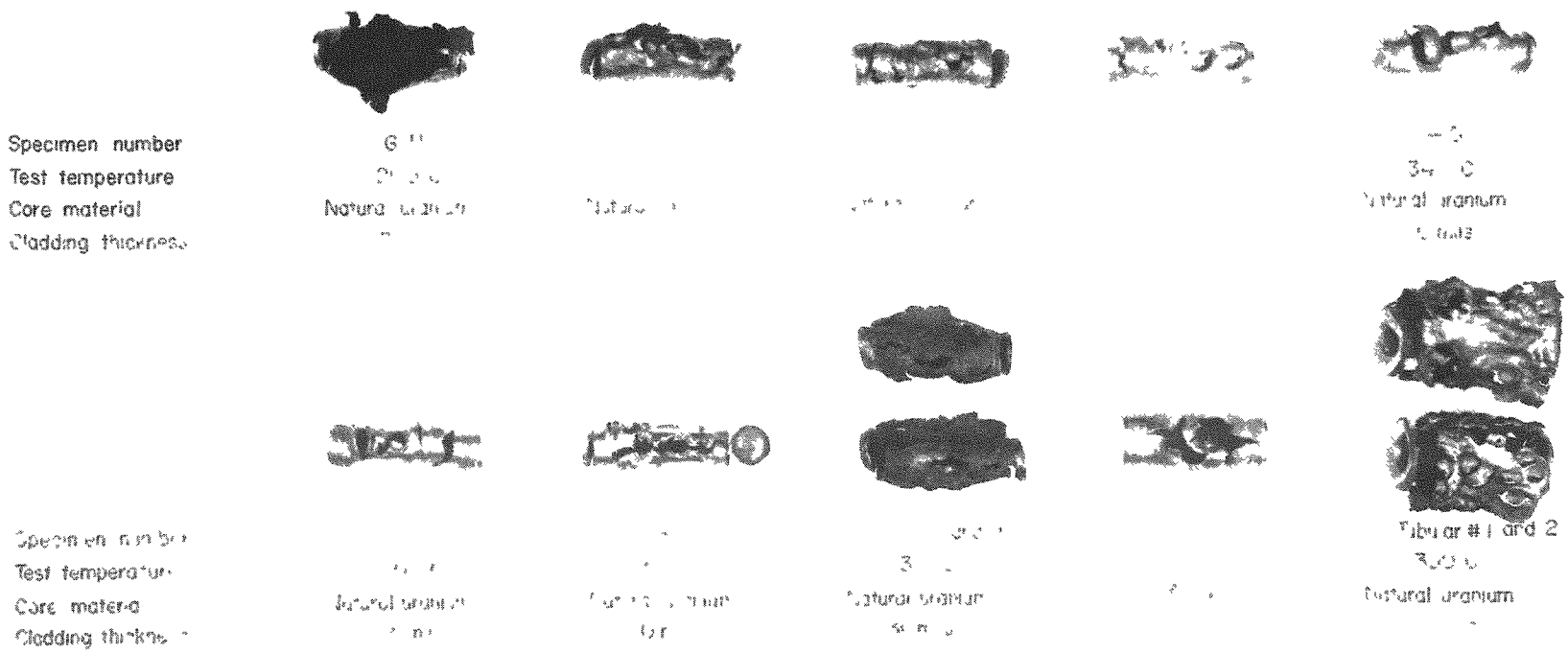

C Specimen Beta treated 720-730 C for 10 minutes, water quenched
D Specimen: Diffusion treated 5.5 hours at 850 C, water quenched.
G and Tubular Specimen Beta treated 720-730 C for 10 minutes; quenched to 590-600 C, held 10 minutes, air cooled.

N61388

FIGURE 7. DEFECTED ZIRCALOY-2-CLAD FUEL SPECIMENS AFTER EXPOSURE IN HOT WATER

(4) Specimens C-8 and C-9, which were beta treated and water quenched, were attacked more rapidly than those cooled at a lower rate.

(5) The most resistant-type element was the diffusion-treated uranium-2 w/o zirconium-core specimen. The induction period was 24 hr before swelling of the cladding occurred, and it was 41 hr before the cladding ruptured.

Reaction-Time Data

The oxidation of the uranium core by the hot water causes hydrogen evolution which increases the pressure of the system. The reaction can be expressed by the equation:

$$U + 2H_2O \rightarrow UO_2 + 2H_2. \quad (1)$$

Pressure-time records of the systems were obtained to provide a more complete understanding of the action of the hot water on defected elements. The records were of value in determining the finish of the reactions and for approximating reaction rates at various times throughout the experiment.

Although the equipment was designed for a maximum pressure of 3000 psi, it was necessary in some experiments to bleed off some of the evolved hydrogen because excessive pressures were reached. In this case, the preheater (Figure 2) was used as additional head space for confining the hydrogen. No pressure-time data were obtained for Experiments 7 and 9B because of a high-temperature leak which allowed some hydrogen to escape. In Experiment 2, a slight leak in a valve allowed some of the water from the reaction vessel to leak into the preheater, creating a variable head space. However, sufficient water remained in the reaction vessel to cover the specimens at all times.

The pressure-time records for the different experiments are plotted in Figures 8 through 17. Table 2 summarizes the data for each experiment. The curves show the total pressure of the system during the run and the pressure due to evolved hydrogen. The hydrogen pressure is the difference between the total pressure and the vapor pressure of the water for that particular experiment. The residual pressures also are given for the systems after the reactions were completed and the vessel had cooled to room temperature. The volume of the head space is shown so that reaction rates can be calculated. The intervals at which hydrogen was bled from the reaction vessel are indicated by the dotted lines in the curves.

The data in Figures 8 through 17 show that the reaction of the core material with the water accelerates rapidly following rupture of the cladding. Although corrosive action is taking place from the time the water covers the specimen, this is not evidenced by gas evolution. It is only after the cladding has ruptured and a considerable area of the core is exposed that the pressure begins to rise. A direct comparison of the different curves should not be made because of variations in head space, hydrogen solubility, temperature, and mode of cracking.

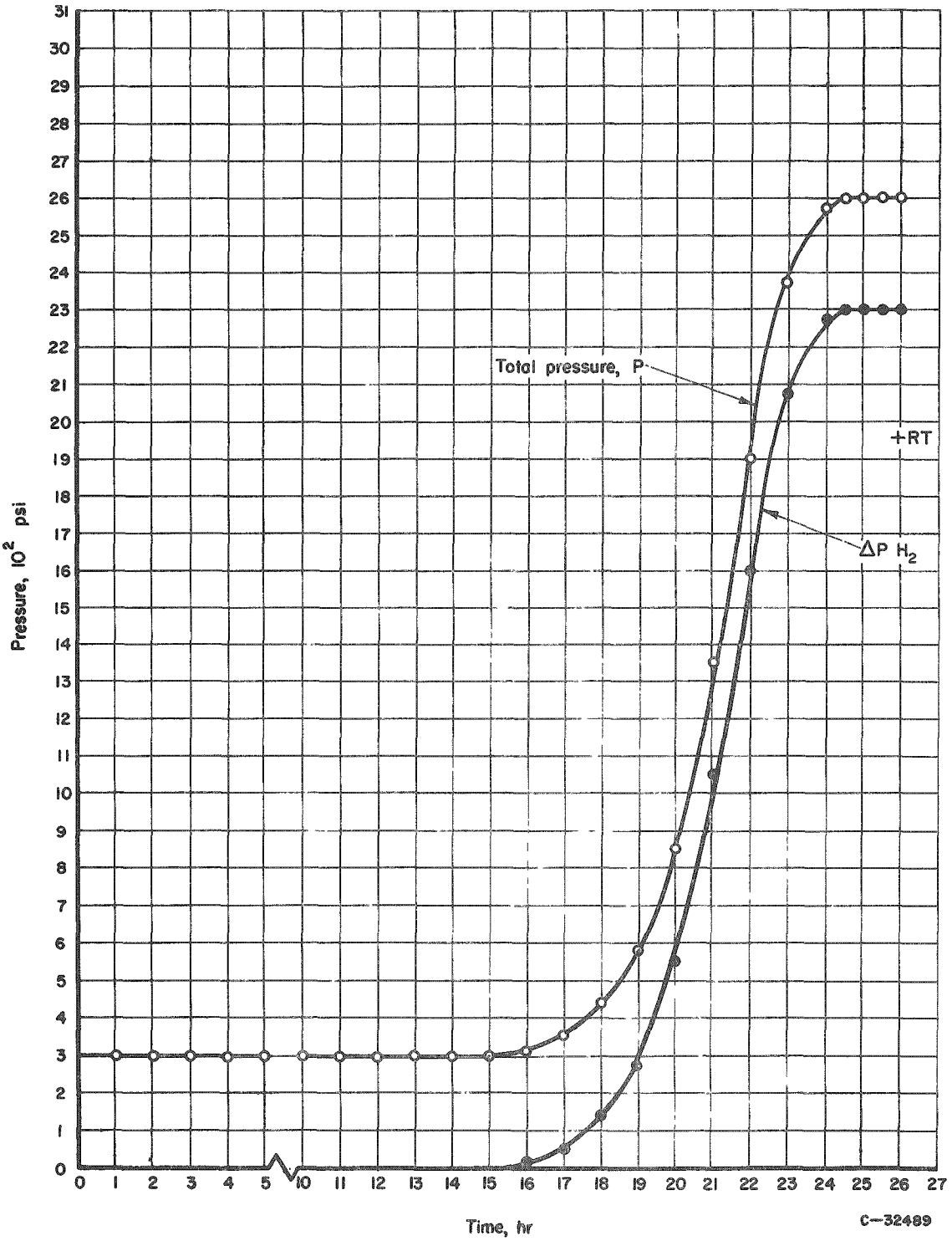

FIGURE 8. PRESSURE-TIME CURVES FOR EXPERIMENT 1

Temperature	200 C
Specimen	G-11
Head space	265 ml

RT is the residual pressure at room temperature after complete reaction.

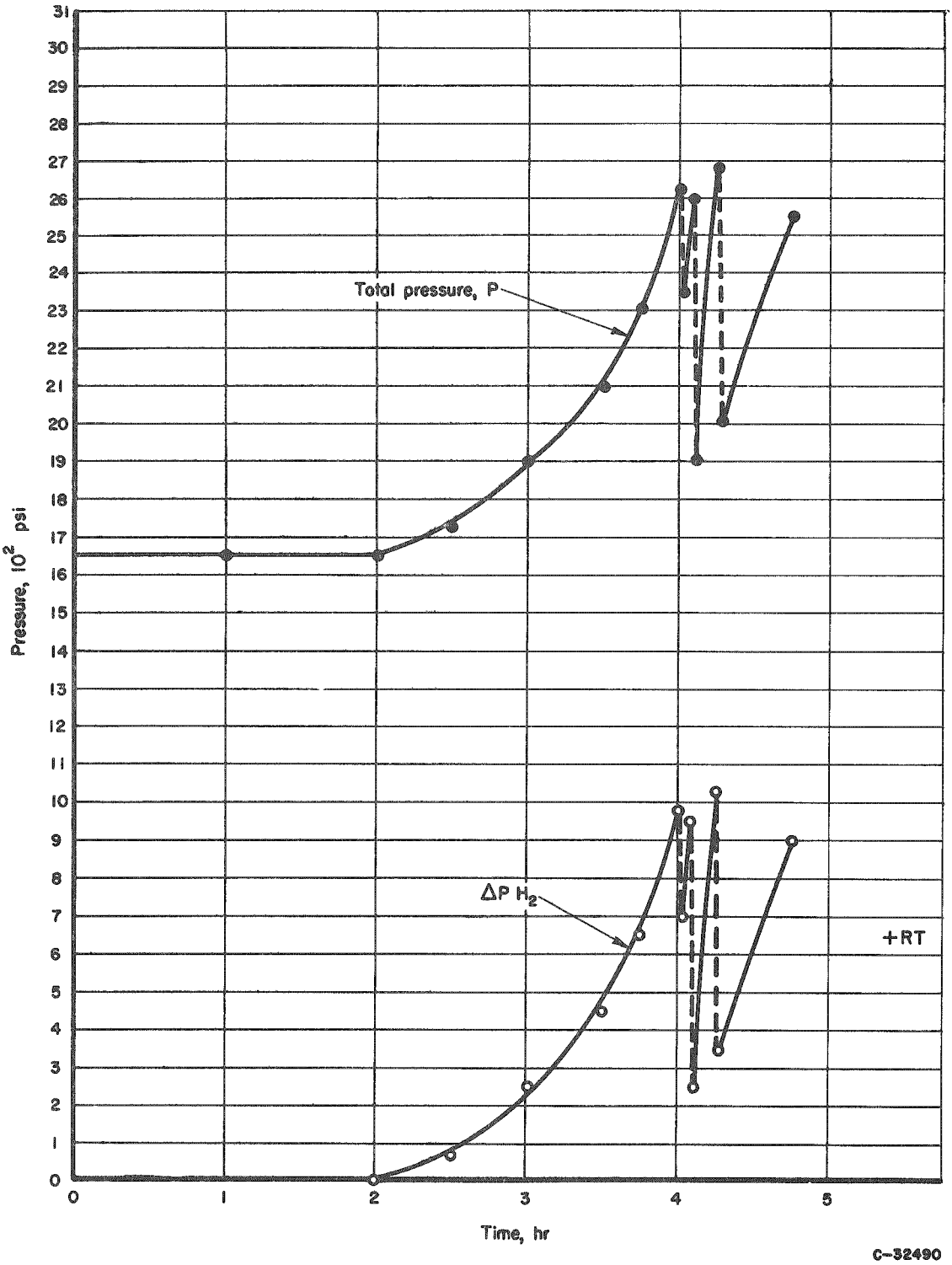

FIGURE 9. PRESSURE-TIME CURVES FOR EXPERIMENT 3A

Temperature	300 C
Specimen	G-14
Head space	Variable

RT is the residual pressure at room temperature after complete reaction.

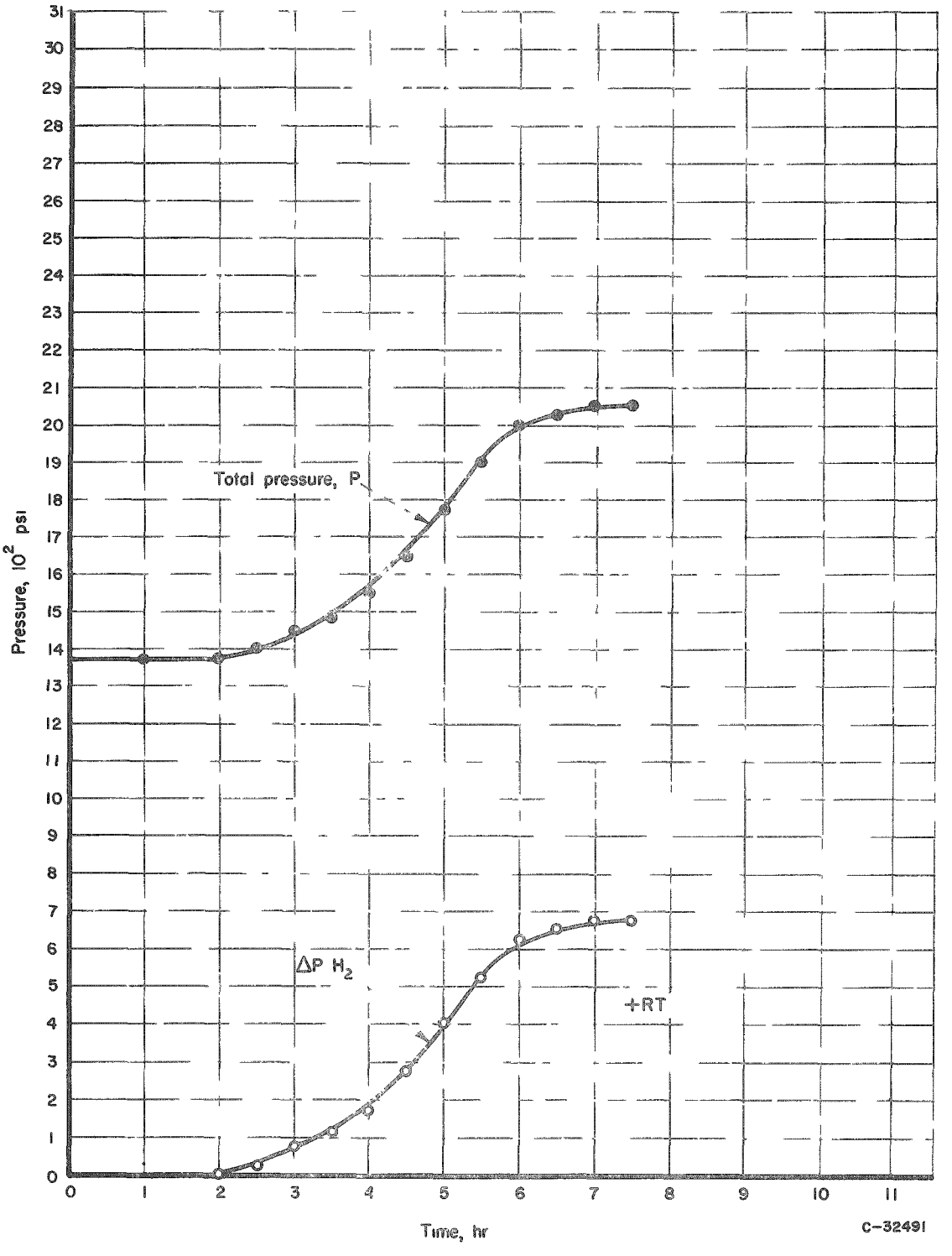

FIGURE 10. PRESSURE-TIME CURVES FOR EXPERIMENT 3B

Temperature	500 C
Specimen	G-22
Head space	1140 ml

PT is the residual pressure at room temperature after complete reaction.

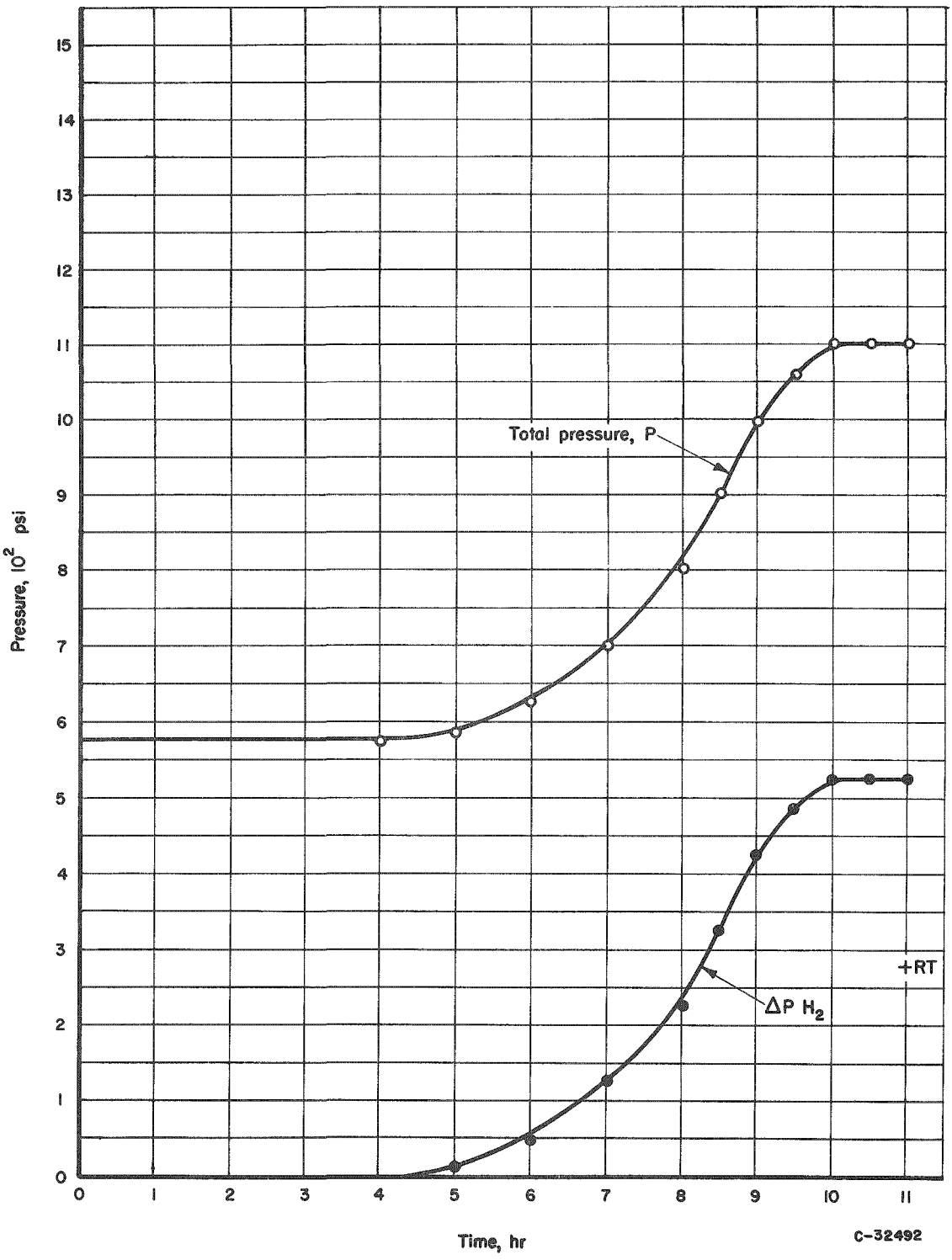

FIGURE 11. PRESSURE-TIME CURVES FOR EXPERIMENT 4

Temperature	250 C
Specimen	G-13
Head space	1100 ml

RT is the residual pressure at room temperature after complete reaction.

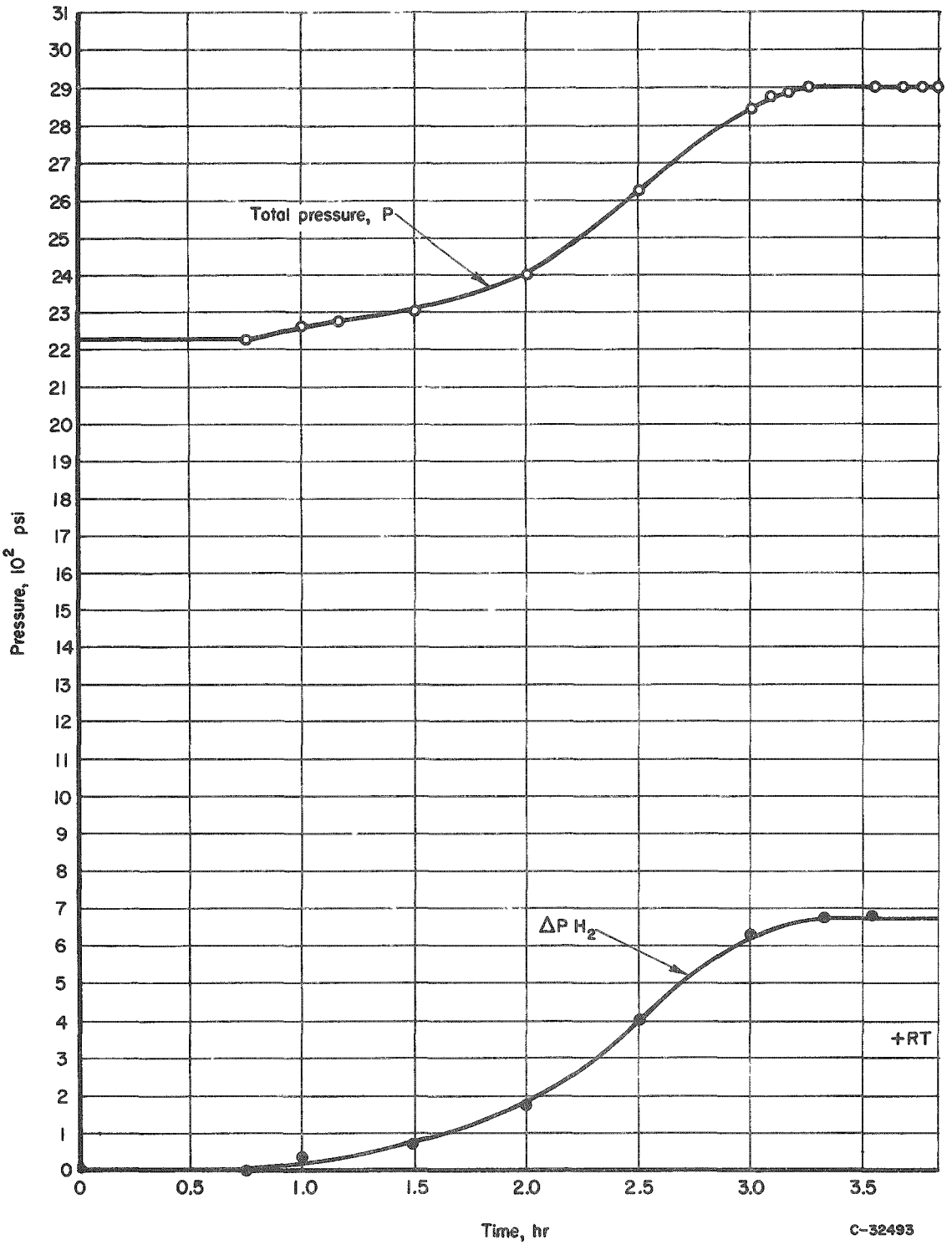

FIGURE 12. PRESSURE-TIME CURVES FOR EXPERIMENT 5

Temperature	345 C
Specimen	G-15
Head space	1200 ml

RT is the residual pressure at room temperature after complete reaction.

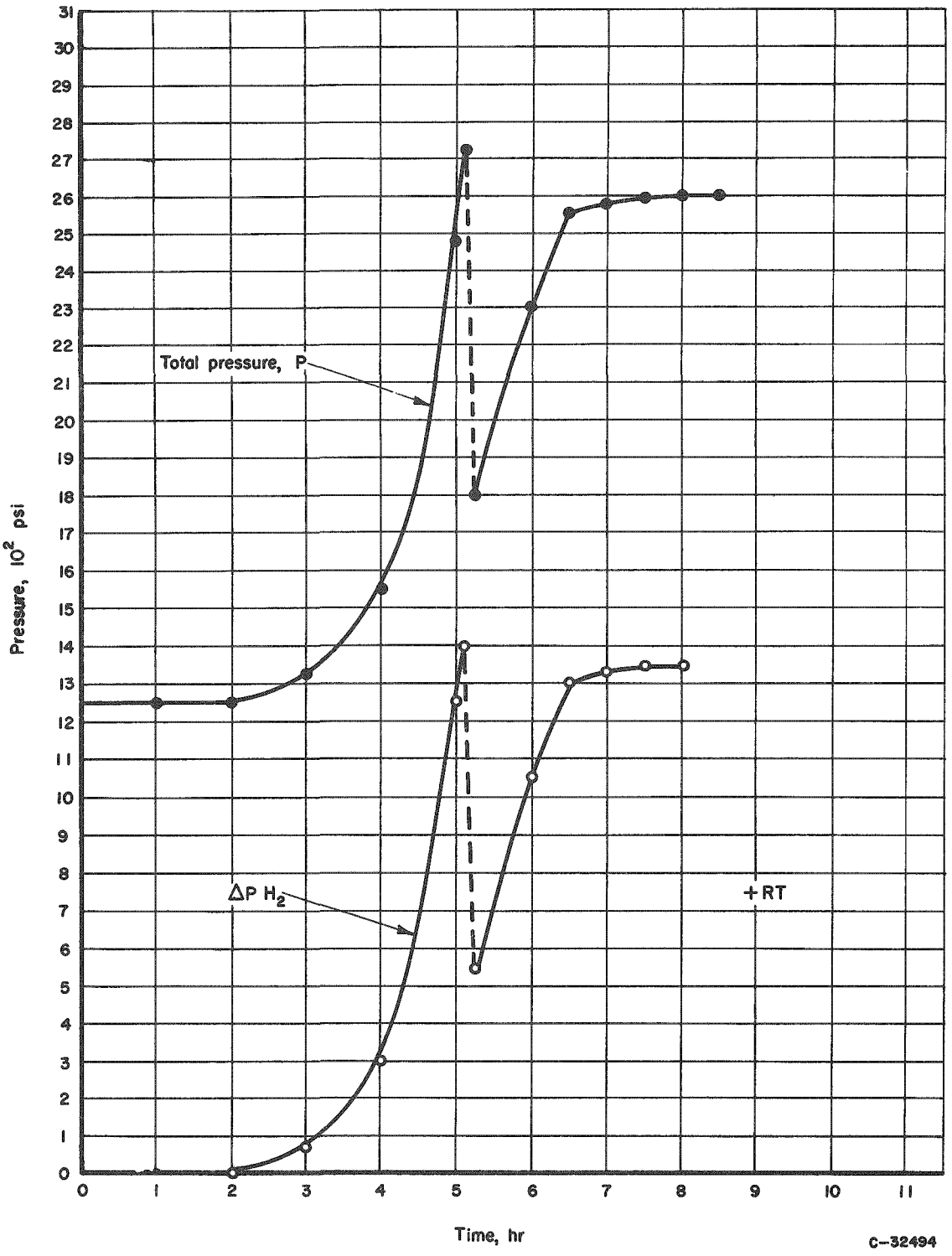

FIGURE 13. PRESSURE-TIME CURVES FOR EXPERIMENT 6

Temperature	300 C
Specimen	G-16
Head space	150 ml for first segment
	1100 ml for last segment

RT is the residual pressure at room temperature after complete reaction.

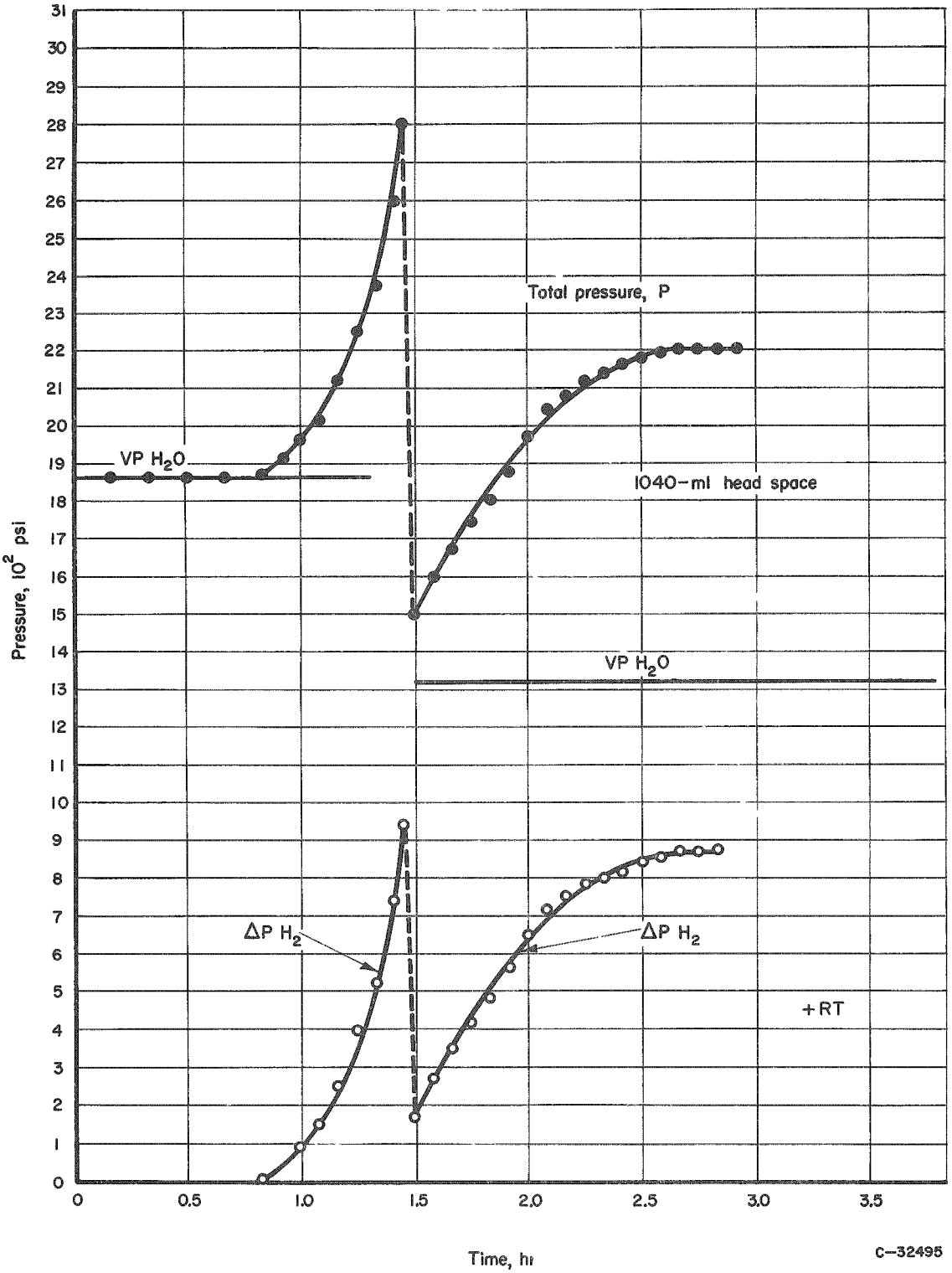

FIGURE 14. PRESSURE-TIME CURVES FOR EXPERIMENT 8

Temperature	300 C
Specimen	C-8
Head space	200 ml for first segment
	1140 ml for last segment

RT is the residual pressure at room temperature after complete reaction.

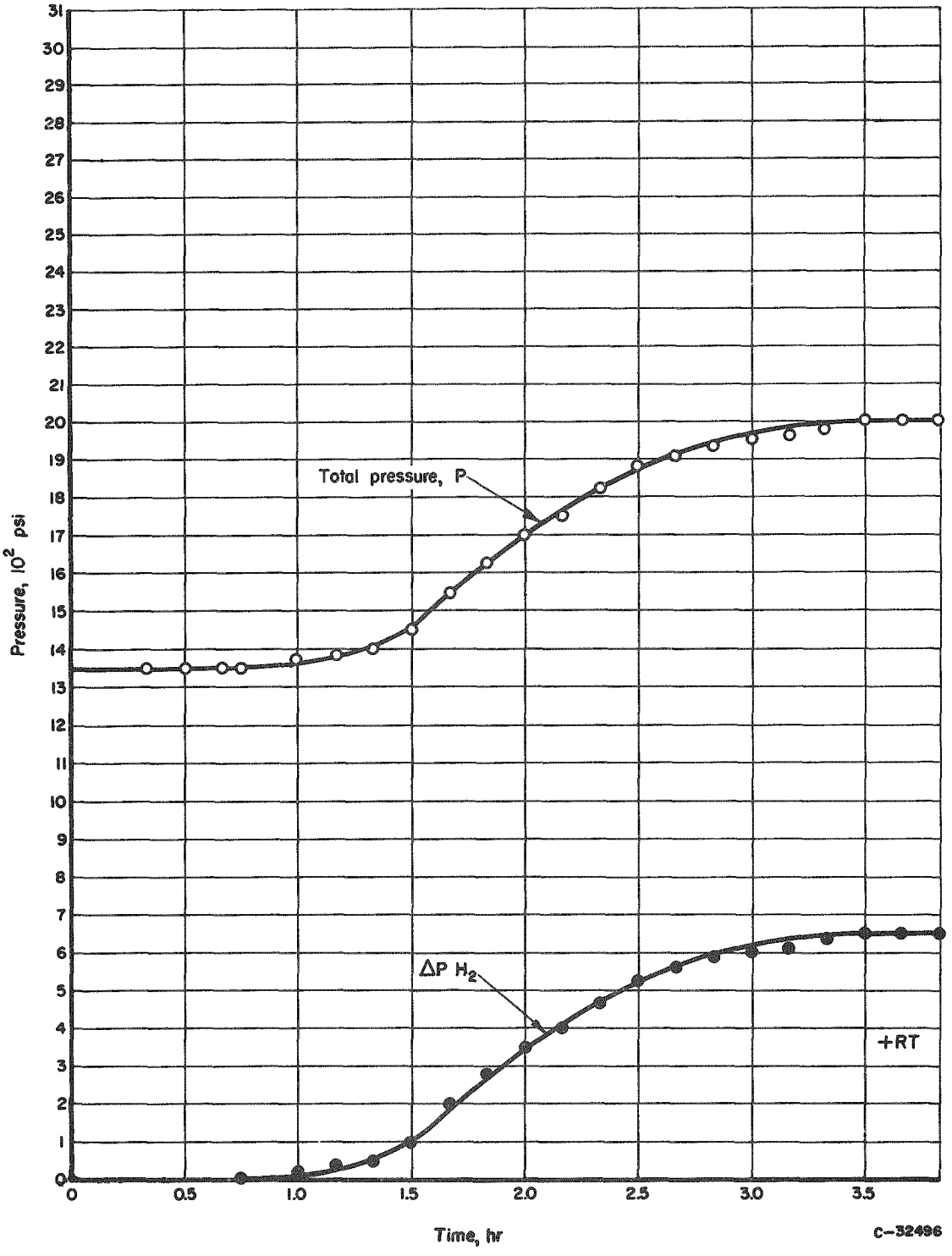

FIGURE 15. PRESSURE-TIME CURVES FOR EXPERIMENT 8B

Temperature	300 C
Specimen	C-9
Head space	1100 ml

RT is the residual pressure at room temperature after complete reaction.

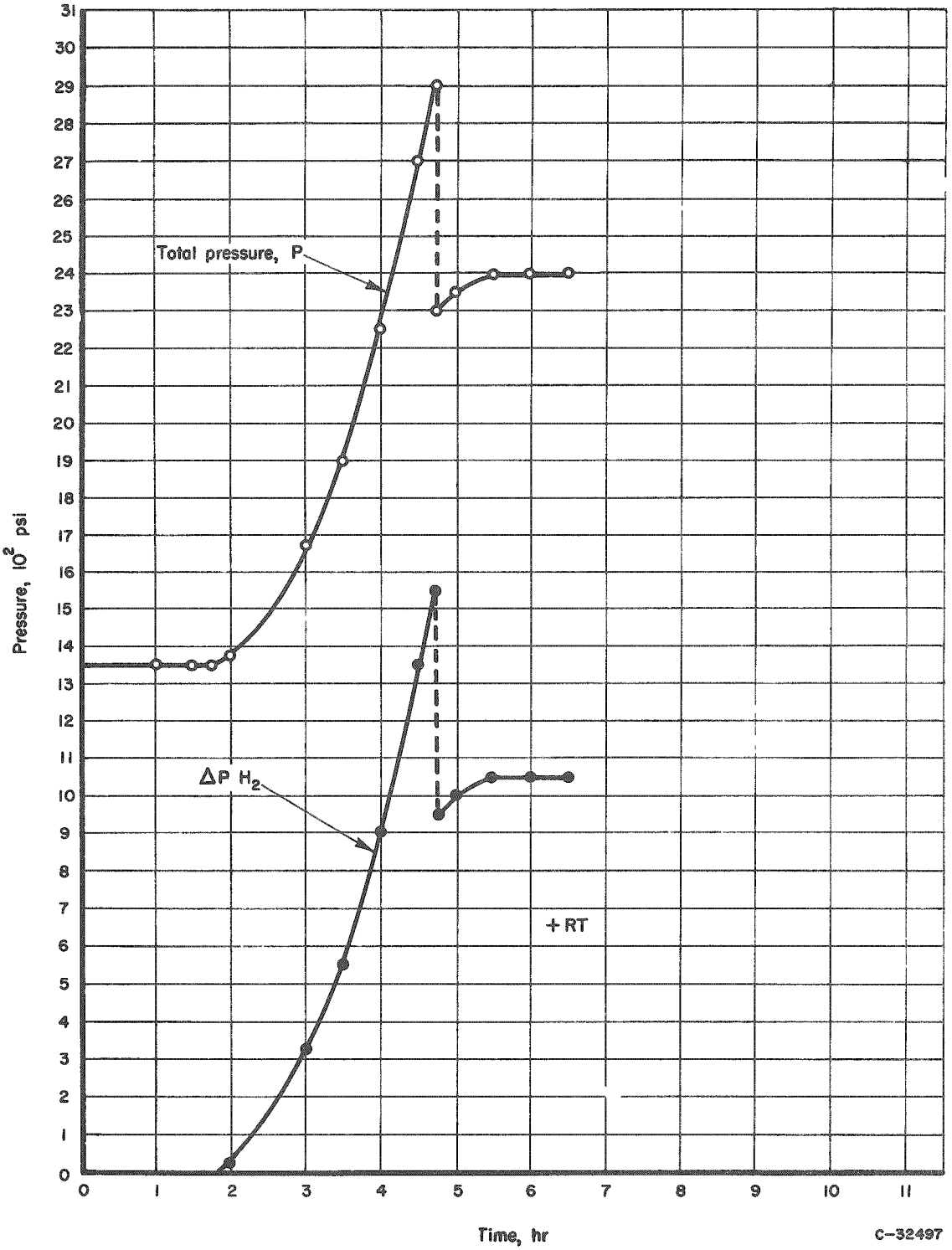

FIGURE 16. PRESSURE-TIME CURVES FOR EXPERIMENT 9

Temperature	300 C
Specimen	Tubular
Head space	1200 ml

RT is the residual pressure at room temperature after complete reaction.

TABLE 3. CALCULATED REACTION RATES BASED ON HYDROGEN EVOLUTION DETERMINED FROM PRESSURE-TIME DATA

Time Interval, hr	Core Reaction Rate, g per hr	Time Interval, hr	Core Reaction Rate, g per hr
Experiment 1, 200 C		Experiment 6, 300 C	
15-17	1.52	2-3	3.53
16-18	2.63	3-4	8.60
17-19	4.61	4-5	28.71
18-20	8.96	5-5.15	36.5
19-21	16.98	5.15-6.0	117.9
20-22	22.99	6.-6.5	109.3
21-23	23.54		
22-24	15.84	Experiment 5, 345 C	
23-24	9.44		
		0.5-1.0	8.82
Experiment 4, 250 C		1.0-1.5	25.04
		1.5-2.0	49.0
4-5	3.23	2.0-2.5	92.2
5-6	6.63	2.5-3.0	122.5
6-7	16.78	3.0-3.5	65.2
7-8	29.43		
8-9	40.35	Experiment 8, 300 C	
9-10	34.79		
		50-60 min	23.88
Experiment 3B, 300 C		60-70 min	36.24
		70-80 min	50.0
2-2.5	10.04	80-87 min	125.6
2.5-3.0	20.30	90-100 min	222.8
3.0-3.5	21.80	101-110 min	176.34
3.5-4.0	22.86	110-120 min	165.48
4.0-4.5	44.64	120-130 min	155.34
4.5-5.0	55.82	130-140 min	144.30
5.0-5.5	57.14	140-150 min	74.28
5.5-6.0	38.54	150-160 min	60.78
6.0-6.5	29.24		
6.5-7.0	19.65		

Generally, after the cladding ruptured, some unreacted core material fell from the specimen into the cold water in the window legs of the reaction vessel. Irregular jagged particles of unreacted core material were often found in the legs when the vessel was opened. Therefore, calculations of core-material balance based on hydrogen evolution (Table 2) show that less reaction occurred than the weight-loss data would indicate.

It should be mentioned that the unreacted metal core particles and the uranium oxide corrosion product could be completely removed from the legs of the autoclave only by dissolution in nitric acid.

According to Equation (1) the hydrogen pressures can be used to estimate the uranium-water reaction rates for the fuel elements under study. The calculations of hydrogen volumes were based on the following assumptions:

(1) The head-space temperature was estimated to be slightly above the reaction-water temperature since some heating was provided in the vapor area.

(2) Hydrogen solubilities in the water were based on temperatures intermediate between the cold-leg temperatures and reaction-water temperatures. Existing solubility data[2] were extrapolated to provide the points needed since actual data are not available.

Calculations were made of reaction rates expressed as grams of uranium per unit of time for some of the experiments. These data, presented in Table 3, show that the rate was greatest for Experiment 8 in which beta-treated water-quenched C-type natural-uranium specimens were used. Note that the time is expressed in minutes for Experiment 8. These results confirm those shown by the photographic studies.

As would be expected, the reaction rates for the same type of element increase with increasing water temperature. It is estimated that the maximum rates obtained in Experiment 8 are similar to what might be predicted for unclad uranium of the same configuration and surface area.

Metallographic Studies

At the completion of Experiment 3, metallographic sections were prepared from the shell of Specimen G-14. One of the sections had a large piece of unreacted core attached to the Zircaloy-2 cladding. Photomicrographs of representative sections of the cladding are presented in Figures 18 and 19.

Of particular interest is the layer formed on the surface of the Zircaloy in contact with the core. It can be seen from Figure 18 that this layer is present only in the areas where the core has completely reacted. Stain-etching techniques indicate that the layer is zirconium hydride. Other than this layer, only scattered hydride needles are visible in the Zircaloy-2.

TABLE 3. CALCULATED REACTION RATES BASED ON HYDROGEN EVOLUTION DETERMINED FROM PRESSURE-TIME DATA

Time Interval, hr	Core Reaction Rate, g per hr	Time Interval, hr	Core Reaction Rate, g per hr
Experiment 1, 200 C		Experiment 6, 300 C	
15-17	1.52	2-3	3.53
16-18	2.63	3-4	8.60
17-19	4.61	4-5	28.71
18-20	8.96	5-5.15	36.5
19-21	16.98	5.15-6.0	117.9
20-22	22.99	6.-6.5	109.3
21-23	23.54		
22-24	15.84	Experiment 5, 345 C	
23-24	9.44		
		0.5-1.0	8.82
Experiment 4, 250 C		1.0-1.5	25.04
		1.5-2.0	49.0
4-5	3.23	2.0-2.5	92.2
5-6	6.63	2.5-3.0	122.5
6-7	16.78	3.0-3.5	65.2
7-8	29.43		
8-9	40.35	Experiment 8, 300 C	
9-10	34.79		
		50-60 min	23.88
Experiment 3B, 300 C		60-70 min	36.24
		70-80 min	50.0
2-2.5	10.04	80-87 min	125.6
2.5-3.0	20.30	90-100 min	222.8
3.0-3.5	21.80	101-110 min	176.34
3.5-4.0	22.86	110-120 min	165.48
4.0-4.5	44.64	120-130 min	155.34
4.5-5.0	55.82	130-140 min	144.30
5.0-5.5	57.14	140-150 min	74.28
5.5-6.0	38.54	150-160 min	60.78
6.0-6.5	29.24		
6.5-7.0	19.65		

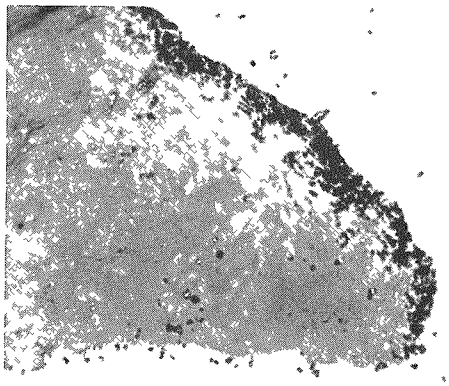

FIGURE 18. PHOTOMICROGRAPH OF SECTION THROUGH THE UNREACTED URANIUM CORE ADHERING TO THE ZIRCALOY-2 CLADDING

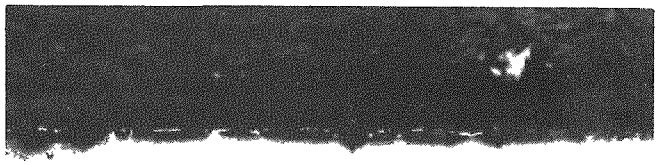

FIGURE 19. PHOTOMICROGRAPH OF CROSS SECTION THROUGH THE FUEL-ELEMENT END PLATE SHOWING THE HYDRIDE LAYER

Based on previous work, one would not expect to find a hydride layer of this type on Zircaloy-2. Normally there is an increase of hydride needles in the Zircaloy-2 matrix without the formation of a distinct layer.

In the case of the defective-fuel-element studies, it would appear that a large concentration of nacent hydrogen from the reaction of water and uranium was in contact with the Zircaloy-2. The reaction was rapid and time was not sufficient to allow significant diffusion of the hydrogen into the matrix of the Zircaloy cladding.

DISCUSSION

The present studies have shown that the failure of defected fuel elements takes place by a series of fairly discrete steps. From a practical standpoint it has been learned that complete failure is not instantaneous after exposure of a defected element to high-temperature water. Rather, an induction period varying from a fraction of an hour to many hours can be anticipated prior to rupture of the cladding, release of hydrogen and gross contamination of the water with radioactive material. Since the time at which each step occurs is dependent on temperature, alloy composition, heat treatment, and configuration, it is not possible to specify definite limitations for a given condition.

At this point, it appears that the initial and final stages of element failure should be studied in greater detail. The present work indicated what might be considered to be clogging of the pinholes in the initial stages. This derives from the fact that, with the possible exception of the experiment at 200 C, neither the pictures nor visual observations revealed any noticeable corrosion products coming from the drilled hole prior to rupture. The significance of this is not clear but may indicate that the detection of cladding failure in a reactor is contingent on rupture of the element and subsequent gross contamination of the water. Thus the warning time would be very short. Additional studies with radioactive material would verify the visual observation that there is no escape of corrosion product through the pinholes.

It may be that consideration should also be given to the design of a mechanical device which would report the slow formation of the blister in the cladding and thus provide warning in sufficient time to shut down the reactor prior to complete rupture of the element.

As was mentioned earlier, the observations of the final stages of failure were obscured by the copious evolution of uranium oxide powder. A dynamic loop system incorporating a porous filter would probably permit continuous observations of the severe tearing and distortion of the cladding as illustrated in the final stages in Figure 7. Such a system would also permit monitoring of the release of radioactive material during the corrosion process.

ACKNOWLEDGEMENT

The authors wish to acknowledge the assistance given them by other Battelle staff members during the program, in particular, the metallographic interpretation received from W. K. Boyd and the helpful suggestions from E. M. Simons and D. R. Grieser.

REFERENCES

(1) Grieser, D. R., and Simons, E. M., "Apparatus for Visual Study of Corrosion by Hot Water", BMI-998 (May 4, 1955).

(2) Stephan, E. F., et al., "Solubility of Gases in Water and Uranyl Salt Solution at Elevated Temperatures and Pressures", BMI-1067 (January 23, 1956).

EFS:PDM:FWF/lfs